Journal of Thermal Analysis, Vol. 49 (1997) 1467-1475

Kinetics

REACTION PATHWAY AND KINETICS OF THE THERMAL DECOMPOSITION OF SYNTHETIC BROCHANTITE

N. Koga[1], *J. M. Criado*[2] *and H. Tanaka*[1]

[1]Chemistry Laboratory, Faculty of School Education, Hiroshima University, 1-1-1 Kagamiyama, Higashi-Hiroshima 739, Japan
[2]Institute de Ciencia de Materiales, C.S.I.C-Universidad de Sevilla, Aptdo. 1115, Sevilla 41071, Spain

Abstract

The reaction pathway of the thermal decomposition of synthetic brochantite, $Cu_4(OH)_6SO_4$, to copper(II) oxide was investigated through the detailed kinetic characterization of the thermal dehydration and desulferation processes. The dehydration process was characterized by dividing into two overlapped kinetic processes with a possible formation of an intermediate compound, $Cu_4O(OH)_4SO_4$. The dehydrated sample, $Cu_4O_3SO_4$, was found first to be amorphous by means of XRD, followed by the crystallization to a mixture of CuO and $CuO{\cdot}CuSO_4$ at around 776 K. The specific surface area and the crystallization behaviour of the amorphous dehydrated compound depend largely on the dehydration conditions. The thermal desulferation process is influenced by the gross diffusion of the gaseous product SO_3, which is governed by the advancement of the overall reaction interface from the top surface of the sample particle assemblage to the bottom.

Keywords: CRTA, DSC, kinetics, synthetic brochantite, TG-DTA, thermal decomposition

Introduction

The decomposition pathway of the thermal decomposition of synthetic brochantite, $Cu_4(OH)_6SO_4$, has not fully been understood as yet because of the dependency on the precipitation and decomposition conditions. Recently, we reported that the title compound with a definite composition can be obtained under the restricted precipitation conditions [1–3]. The sample was decomposed thermally to copper(II) oxide via a dehydrated amorphous intermediate, $Cu_4O_3SO_4$, with the three distinguished thermal behaviours: (1) thermal dehydration, (2) in-situ crystallization of dehydrated amorphous compound, and (3) thermal desulferation [1–3]. The decom-

0368–4466/97/ $ 5.00

John Wiley & Sons Limited
Chichester

position pathway determined by the thermoanalytical (TA) measurements complemented by the results of X-ray powder diffractometry (XRD), FT-IR spectroscopy, and chemical analyses of Cu^{2+} and SO_4^{2-} was in good agreement with the previously reported results for the reaction under flowing N_2 [4–6]. Alternative reaction mechanism has been proposed on the basis of the thermogravimetric analyses with fairly large sample mass, several hundreds mg, under static air [7], where the sample decomposes in two steps via $Cu_4O(OH)_4SO_4$. It is expected that the detailed kinetic study of the respective reaction steps helps us to understand the reaction pathway and mechanism of the thermal decomposition of the title compound.

In the present study, the respective thermal behaviours in the decomposition pathway proposed by us are interpreted kinetically by means of the TA techniques complemented by XRD, FT-IR and microscopic observations. The possible reason for the different reaction pathway proposed is discussed on the basis of the kinetic information.

Experimental

Sample preparation

Precipitates of basic copper(II) sulfate were obtained at 298 K by adding 0.1 *M* NaOH solution dropwise at a rate of 1.0 ml min^{-1} with stirring to 100 ml of 0.1 *M* $CuSO_4$ solution until the *pH* of the resulting solution was equal to 8.0 [1, 2]. The precipitates, dried in air and ground in an agate mortar, were characterized by means of XRD, FT-IR and TG and was identified as corresponding to the mineral brochantite $Cu_4(OH)_6SO_4$.

Thermal dehydration

The sample of 10.0 mg, sieved to –170+200 mesh fraction, was weighed into a platinum crucible of 5 mm in diameter and 2.5 mm in depth. TG-DTG and TG-DTA curves were recorded simultaneously at various heating rates $1.0 \leq \Phi \leq 10.0$ K min^{-1} in a flow of N_2 at a rate of 30 ml min^{-1}, using Shimadzu TGA-50 and ULVAC TGD-9600 apparatuses. DSC curves were obtained using a silver crucible in ULVAC DSC-9400 under the conditions otherwise identical with the TG runs. It is known that the thermal dehydration proceeds through the following two overlapping processes [1, 2, 5, 6, 8].

$$Cu_4(OH)_6SO_4 \rightarrow Cu_4O(OH)_4SO_4 + H_2O \quad (1)$$

$$Cu_4O(OH)_4SO_4 \rightarrow Cu_4O_3SO_4 + 2H_2O \quad (2)$$

The intermediate compound $Cu_4O(OH)_4SO_4$ was prepared by heating 10.0 mg of the sample at 528 K for 15 h in Shimadzu TGA-50 apparatus. After cooling down the sample to room temperature in the atmosphere of nitrogen flow, the intermediate compound was heated up to 773 K under the condition identical to the above TG

measurements in order to initiate the second reaction. TG curves for the first reaction at various heating rates were obtained by subtracting the TG curve for the second reaction from that of the overall dehydration.

In-situ crystallization

For preparing the dehydrated sample, 500 mg of the sample were heated up to 763 K in flowing N_2 at a rate of 50 ml min^{-1} using an apparatus of the CRTA constructed with a thermobalance of Ci Robal. The dehydration rate C was controlled to keep various constant rates $0.01 \leq C \leq 0.24$ mg min^{-1}. The dehydrated sample was identified by the XRD and FT-IR, and was measured its specific surface area by the BET method. 10.0 mg of the dehydrated samples were weighed into an alumina crucible and subjected to the DSC measurements in flowing He at a rate of 30 ml min^{-1}, using an instrument from SETARAM.

Thermal desulferation

The kinetic curves for the isothermal desulferation reaction at various temperatures $843 \leq T \leq 900$ K were recorded on Shimadzu TGA-50 in flowing N_2 at a rate of 30 ml min^{-1} using 10.0 mg of the sample, which were heated up to the predetermined constant temperature at a rate of 20 K min^{-1}. The non-isothermal desulferation process was also recorded at various heating rates $1.0 \leq \Phi \leq 10.0$ K min^{-1} under the conditions otherwise identical with the isothermal run.

Results and discussion

Typical TG-DTA and DSC curves for the thermal decomposition of synthetic brochantite to copper(II) oxide is shown in Fig. 1. The mass loss due to the dehydration completes at 700 K. The subsequent exotherm corresponds to the crystallization of the amorphous dehydrated product, followed by the endothermic desulferation reaction.

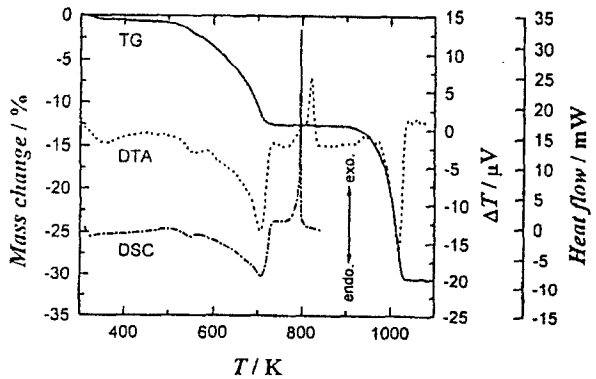

Fig. 1 Typical TG-DTA and DSC curves for the thermal decomposition of synthetic brochantite at a heating rate of 10 K min^{-1}

Thermal dehydration

Under linearly increasing temperature, the dehydration process indicates an anomaly in the DTA and DSC curves. When the sample were heated isothermally in the temperature range of $510 \leq T \leq 540$ K, the dehydration reaction takes place with the mass loss corresponding quantitatively to Eq. (1). The IR absorption bands due to OH and SO_4 groups remain unchanged virtually even with the loss of two OH groups, as was already clarified by Secco [8]. The thermal decomposition of the intermediate compound proceeds in the temperature range of $570 \leq T \leq 720$ K, characterized by the well distinguished single peak of DTA and DTG with the mass-loss corresponding quantitatively to Eq. (2). The IR absorption bands due to OH groups disappear after completion of the reaction step [1, 2]. The dehydrated compound, $Cu_4O_3SO_4$, was amorphous in view of XRD, supported by the broad IR absorption band due to SO_4 group in the range of 600–1100 cm^{-1}.

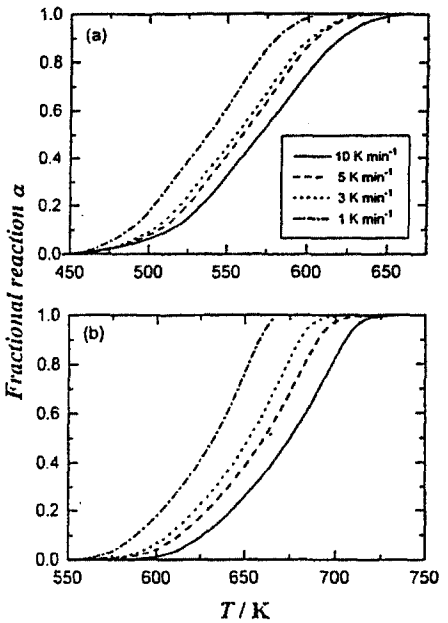

Fig. 2 Typical non-isothermal kinetic curves for the thermal dehydration of synthetic brochantite; a) $Cu_4(OH)_6SO_4 \rightarrow Cu_4O(OH)_4SO_4 + H_2O$, b) $Cu_4O(OH)_4SO_4 \rightarrow Cu_4O_3SO_4 + 2H_2O$

Typical plots of the fractional reaction α *vs.* T for the respective dehydration steps obtained by the experimental treatment described above are shown in Fig. 2. The apparent activation energy E at various α were calculated from the Friedman method [9] by plotting $\ln(d\alpha/dt)$ *vs.* T^{-1} at a given α. The constant E values of 158.0 ± 1.3 and 193.1 ± 0.9 kJ mol^{-1} were obtained for the first and second reactions in the ranges of $0.2 \leq \alpha \leq 0.8$ and $0.1 \leq \alpha \leq 0.9$, respectively. The kinetic rate data were extrapolated to infinite temperature using the E values averaged over the restricted α range, according to the Eq. (3) [10, 11]:

$$\frac{d\alpha}{d\theta} = \frac{d\alpha}{dt} \exp\left(\frac{E}{RT}\right) = Af(\alpha) \tag{3}$$

where θ is the generalized time [12] denoting the reaction time at infinite temperature. Figure 3 shows the plots of $d\alpha/d\theta$ and θ against α as the kinetic curves at infinite temperature. From the detailed analyses of the kinetic curves at infinite temperature [13], the Avrami-Erofeev A_m type equation, $m(1-\alpha)[-\ln(1-\alpha)]^{1-1/m}$, with $m=0.5$ and the diffusion controlled interface shrinkage D_n type equation, $[(1-\alpha)^{2/n-1}-1]^{-1}$, with $n=2.6$ were selected as the most appropriate kinetic model functions for the first and second dehydration steps, respectively. Table 1 summarizes the apparent kinetic results for the dehydration processes.

It is apparent that the respective reaction steps of the dehydration are controlled by the different kinetics. The interface shrinkage type reaction controlled by the diffusional removal of the evolved water vapor estimated for the second reaction step seems to be influenced by the atmospheric and/or self-generated water vapor. The kinetic findings are also supported by the reported experimental evidence [14] that the removal of evolved water is difficult due to the possible formation of the zeolite type water. Accordingly, the higher water vapor pressure during the dehydration processes seems to be responsible for the formation of stable $Cu_4O(OH)_4SO_4$ reported by Prasad and Rao [7].

In-situ crystallization

In CRTA, the sample was dehydrated quantitatively to $Cu_4O_3SO_4$, which did not indicate any distinguished diffraction peaks by XRD irrespective of the dehydration

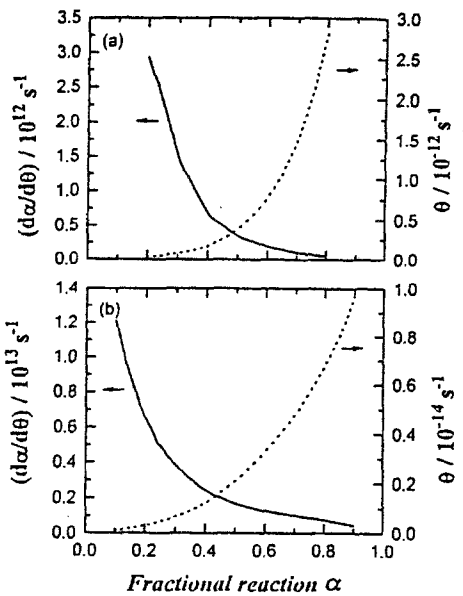

Fig. 3 Typical plots of $d\alpha/d\theta$ and θ *vs.* α for the thermal dehydration of synthetic brochantite; a) $Cu_4(OH)_6SO_4 \rightarrow Cu_4O(OH)_4SO_4 + H_2O$, b) $Cu_4O(OH)_4SO_4 \rightarrow Cu_4O_3SO_4 + 2H_2O$

Table 1 The apparent kinetic parameters for the non-isothermal dehydroxylation of the synthetic brochantite

Reaction	Range of α	E/kJ mol^{-1}	$f(\alpha)$	Exponent	A/s^{-1}
Eq. (1)	$0.2 \leq \alpha \leq 0.8$	158.0±1.3	$m(1-\alpha)[-\ln(1-\alpha)]^{1-1/m}$	$m=0.5$	1.79×10^{12}
Eq. (2)	$0.1 \leq \alpha \leq 0.9$	193.1±0.9	$[(1-\alpha)^{2/n-1}-1]^{-1}$	$n=2.6$	3.28×10^{11}

Table 2 Influence of the dehydroxylation rate C in the CRTA on the specific surface area S and the crystallization behaviour of the amorphous dehydroxylated sample

C/mg min^{-1}	S/m^2(g $Cu_4O_3SO_4$)$^{-1}$	$T_{e.o.}$*1/K	T_p*2/K	ΔH/J(g $Cu_4O_3SO_4$)$^{-1}$
6.7×10^{-2}	11.2	776.5±0.2	839.7±0.2	−139.1±1.8
9.0×10^{-2}	9.2	776.0±0.2	839.3±0.2	−134.5±1.6
1.2×10^{-1}	8.1	776.0±0.2	839.1±0.2	−129.1±1.5
2.4×10^{-1}	6.8	775.7±0.2	838.7±0.2	−111.1±1.3

*1Extrapolated onset temperature on the DSC curves at 10 K min^{-1}

*2Peak top temperature on the DSC curves at 10 K min^{-1}

rate. It was confirrned by XRD that the amorphous dehydrated product crystallizes to CuO and $CuO{\cdot}CuSO_4$, with well distinguished single exothermic peak in DSC (Fig. 1). Table 2 lists the effect of the dehydration rate on the specific surface area of the amorphous product, together with the DSC profiles of the crystallization process. It is clearly seen that the specific surface area and the enthalpy change ΔH due to the crystallization decrease with increasing the dehydration rate. It is expected from the present results that the state of amorphous dehydrated sample is influenced by the rate, temperature and/or atmospheric conditions during the dehydration.

Thermal desulferation

Figure 4 shows the typical kinetic curves for the thermal desulferation of $Cu_4O_3SO_4$ under the isothermal and linearly increasing temperature conditions. The isothermal kinetic curves are characterized predominantly by the monotonous reaction rate. The α dependence of the apparent E value evaluated by the Friedman plots was shown in Fig. 5. The values of E are approximately constant during the course of reaction with the mean values 259.1±3.4 and 252.6±6.2 kJ mol^{-1} for the isothermal and non-isothermal desulferation processes, respectively. Figure 6 shows the kinetic rate data at infinite temperature as the plots of $d\alpha/d\theta$ against α. Irrespective of the isothermal or non-isothermal reaction conditions, the reaction proceeds with the constant rate until α reaches around 0.6, followed by the slight

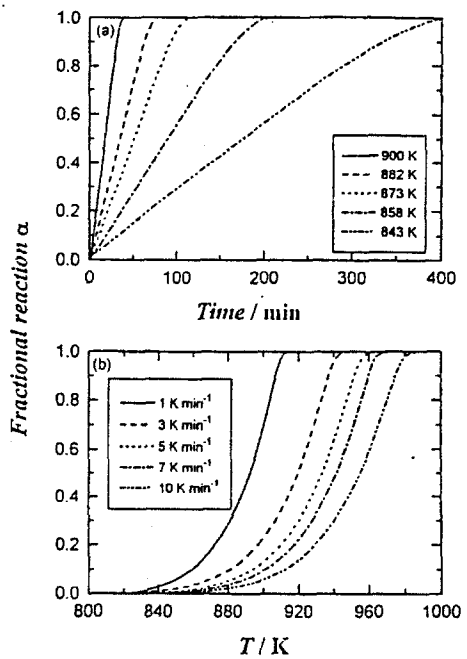

Fig. 4 Typical kinetic curves for the thermal desulferation of $Cu_4O_3SO_4$ under a) isothermal and b) non-isothermal conditions

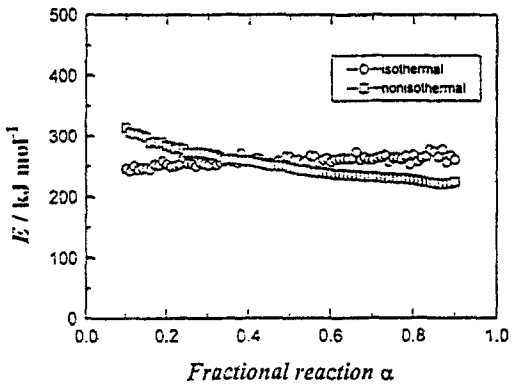

Fig. 5 The α dependence of the apparent values of E for the thermal desulferation of $Cu_4O_3SO_4$

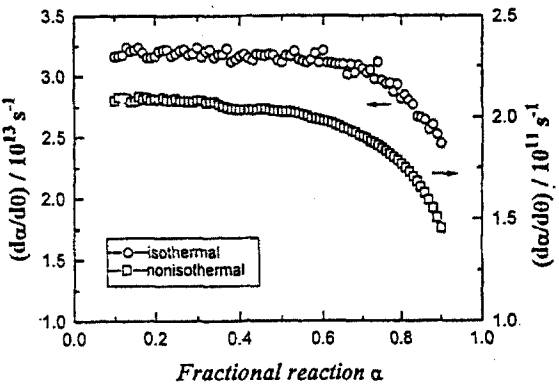

Fig. 6 The plots of $d\alpha/d\theta$ *vs.* α for the thermal desulferation of $Cu_4O_3SO_4$

decrease in the rate in the later reaction stages. It is worth noting that the apparently larger rate was observed for the isothermal desulferation.

The constant desulferation rate during the first half of the reaction indicates that the overall reaction interface advances from the top surface of the sample particle assemblage in the crucible to the bottom. The concentration gradient of the evolved gas is one of the probable reason for this type of overall reaction behaviour. The rate of reaction interface advancement is thus influenced by the gross diffusion of evolved SO_3. The lower reaction rate at infinite temperature under non-isothermal condition may result from the higher partial pressure of the self-generated SO_3.

It was recognized from the SEM observation that the sintering of the solid product CuO initiates already during the course of the desulferation, resulting consequently the volume shrinkage of the sample assemblage. The gradual decrease in the value of $d\alpha/d\theta$ at the later half of the reaction is explained in connection with the difficulty of the gross diffusion of the evolved SO_3 through the sintered product layer.

References

1 H. Tanaka and N. Koga, Thermochim. Acta, 133 (1988) 221.
2 H. Tanaka and N. Koga, J. Chem. Educ., 67 (1990) 612.
3 H. Tanaka, M. Kawano and N. Koga, Thermochim. Acta, 182 (1991) 281.
4 G. Pannetier, J. M. Bregeault, G. Djega-Marladassou and M. Grandon, Bull. Soc. Chim. France, (1963) 2616.
5 E. V. Margulis, Russ. J. Inorg. Chem., 7 (1962) 935.
6 P. Ramamurthy and E. A. Secco, Can. J. Chem., 48 (1970) 3510.
7 S. V. S. Prasad and V. S. Rao, J. Thermal Anal., 30 (1985) 603.
8 E. A. Secco, Can. J. Chem., 66 (1988) 329.
9 H. L. Friedman, J. Polym. Sci. C, 6 (1964) 183.
10 T. Ozawa, J. Thermal Anal., 31 (1986) 547.
11 N. Koga, Thermochim. Acta, 258 (1995) 145.
12 T. Ozawa, Bull. Chem. Soc. Jpn., 38 (1965) 1881; J. Thermal Anal., 2 (1970) 301; Thermochim. Acta, 100 (1986) 109.
13 N. Koga and J. Malek, Thermochim. Acta, 283 (1996) 69.
14 I. Uzunov, D. Klissurski and L. Teocharov, J. Thermal Anal., 44 (1995) 685.